ACS APPLIED MATERIALS & INTERFACES

Research Article

www.acsami.org

A Perylene Diimide Crystal with High Capacity and Stable Cyclability for Na-Ion Batteries

Wenwen Deng, Yifei Shen, Jiangfeng Qian, Yuliang Cao, and Hanxi Yang*

College of Chemistry and Molecular Science, Wuhan University, Wuhan 430072, China

S *Supporting Information*

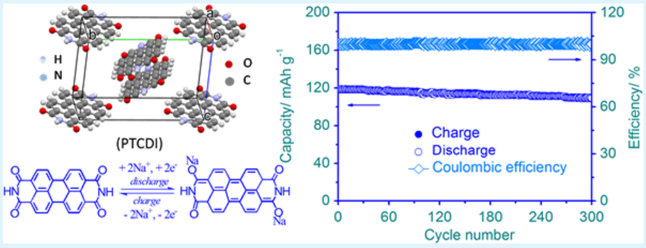

ABSTRACT: Organic Na-host materials have are now actively pursued as an attractive alternative to conventional transition-metal compounds for development of sustainable sodium ion batteries; however, most of the organic compounds reported so far suffer from their low reversible capacity and poor cyclability. Here, we report a simple perylene diimide, 3,4,9,10-perylene-bis(dicarboximide) (PTCDI), which demonstrates remarkable electrochemical performances as an organic cathode for Na-ion batteries. With the high density of redox-active carbonyl groups in a stable π-conjugated structure, the PTCDI molecule can undergo a two-electron redox reaction with reversible insertion/extraction of 2 Na^+ ions per molecular unit, demonstrating a high capacity of 140 mAh g^{-1}, a strong rate performance with a reversible capacity of 103 mAh g^{-1} at 600 mA g^{-1} (5 C,1 C = 120 mA g^{-1}) and a long-term cyclability with 90% capacity retention over 300 cycles. Because this PTCDI material is commercially available and nontoxic, it may serve as a new alternative cathode for Na-ion battery applications.

KEYWORDS: *sodium ion batteries, organic cathode, Na-host material, perylene diimide, electrochemical enolization reaction*

INTRODUCTION

Sodium-ion batteries (SIBs) have recently aroused considerable interest as a low cost alternative to Li-ion batteries for electric energy storage applications because of the natural abundance of sodium resources and the similar intercalation chemistry of sodium ions with lithium ions.[1−3] Though a large variety of Na-insertion compounds with acceptable electrochemical performances have been reported as possible cathode-active materials for SIBs, they are mostly based on transition-metal compounds,[4,5] which will still impose cost and resource restraints for large scale applications. Therefore, development of low cost and "rare metal-free" electrodes is of practical importance to promote Na-ion batteries for widespread electric storage applications.

In recent development of organic materials for Na-ion batteries, a variety of redox-active polymers have been reexamined as Na cathode hosts due to their flexible frameworks and tunable redox potentials.[6] Though a few of p-doped polymers[7−10] and radical polymers[11] demonstrated a high potential and redox activitiy in Na-ion battery electrolytes, their charge/discharge reactions took place through a reversible p-doping/dedoping mechanism of electrolyte anions, which cannot act as a Na^+ host for Na-ion batteries. Recently, a number of self-doped polymers with ionizable sodium sulfonate[12,13] and tailored aromatic polyimides with Na^+-associable carbonyl groups[14,15] were found to reversibly accommodate Na^+ ions as organic cathodes; however, their Na-storage capacities are not sufficiently high due to their low densities of active sites for the electrochemical sodiation reaction in the large polymeric backbones.

In principle, many small organic molecules with carbonyl groups, such as quinones, anhydrides, imides, and ketones, can undergo electrochemical redox reactions through reversible uptake and release of alkali ions at considerably high potentials, possibly serving as high capacity organic cathodes for battery applications. However, these organic compounds are mostly investigated as Li- storage cathodes[16−19] but have been less examined in Na^+ electrolytes. Recently, Yao et al. reported a 5,5′-indigodisulfonic acid sodium salt with a discharge capacity of ~90 mA g^{-1} at 1.8 V (vs Na^+/Na) and a stable cyclability in Na^+ electrolyte.[20] Similar Na-storage behaviors were also observed for disodium pyromellitic diimidate.[21] Particularly, Luo et al. reported a commercially available organic pigment, 3,4,9,10-perylene-tetracarboxylicacid-dianhydride, as Na-ion battery cathode, which demonstrated a high capacity of 145 mAh g^{-1}, high rate capability up to 1000 mA g^{-1}, and stable cycling performance over 200 cycles.[22] Nevertheless, these pioneering works have revealed the feasibility to build high-capacity and cycle-stable Na-storage cathodes using small organic molecules.

In the search for better organic cathodes for Na-ion batteries, we focused our attention on perylene diimide compounds because of their insolubility in organic electrolytes and multiple Na^+-bonding sites per molecular unit, which are critical for an organic cathode to achieve a long cycle life and high Na-storage capacity. Among the perylene diimide derivatives tested, a

Received: May 19, 2015
Accepted: September 11, 2015
Published: September 11, 2015

structurally simplest 3,4,9,10-Perylene-bis(dicarboximide) (PTCDI) exhibits a high reversible capacity of 140 mAh g^{-1} and a remarkable capacity retention of 90% over 300 cycles. Particularly, this molecule is commercial available and nontoxic, possibly fulfilling the needs for large-scale battery applications. Here, we report the electrochemical behavior of PTCDI as an organic cathode and describe its Na-storage mechanism in organic electrolyte.

■ EXPERIMENTAL SECTION

The PTCDI sample used in this was commercially available product (97% purity), purchased from Chushenwei Chemical Industry Co., Ltd., Hubei, China, and used without further purification. The organic cathode was prepared by mixing 70% PTCDI powders, 20% Super P carbon and 10% polytetrafluoroethylene binder into an electrode paste, then rolling the paste into a thin film of ~100 μm thickness and finally pressing the electrode film onto an aluminum mesh. The electrochemical performances of the PTCDI cathode were evaluated by 2016 type coin cells using a Na disk as anode, a porous polypropylene separator (Celgard No. 2400, Celgard, Inc.) as separator and 1.0 mol L^{-1} $NaPF_6$ in a mixed solvent of ethylene carbonate (EC), diethylcarbonate (EC) and propylene carbonate (PC) (EC/DEC/PC, 45:45:10 vol %) as electrolyte. Each cathode contained approximately 3 mg active PTCDI powers. All the coin cells were assembled in a glovebox with water/oxygen content lower than 1 ppm and tested at room temperature. The galvanostatic discharge/charge tests were conducted on a LAND cycler (Wuhan Kingnuo Electronic Co. China). Cyclic voltammetric measurements were performed at a scan rate of 1 mV s^{-1} on a CHI 660a electrochemical workstation (Chen Hua Instruments Co., China).

The morphologies of the PTCDI material were observed by using SEM (Sirion, 2000, FEI) and TEM (JEM-2010FEF). The FTIR spectrum was recorded using KBr pellets on AVATAR 360 spectrometer (Nicolet Instrument Corp., Madison, WI) in wavelength range of 400−4000 cm^{-1}. The lattice structure of the PTCDI crystal was analyzed by powder X-ray diffraction in the 2θ range of 5−80° at a scan rate of 4° min^{-1} on a Shimadzu XRD-6000 diffractometer with Cu Kα. XRD peaks of PTCDI was analyzed using Jade 6.5 software. For these ex situ spectroscopic characterizations, the test cells were disassembled in Ar-filled glovebox (O_2 and H_2O concentration <1.0 ppm) and the cathode samples were peeled off from the current collector, repeatedly rinsed with pure DEC solvent and then vacuum-dried at 100 °C for 40 min. The prepared cathode samples were immediately sent for XRD measurements. The schematic diagram of the molecular arrangement in PTCDI crystal was analyzed using the Materials module within Mercury CSD 2.0.[23]

For quantitative determination of the Na contents in the cycled cathodes, the cathode samples disassembled from the coin cells at different charge/discharge depths was rinsed several times with pure EC solvent and then burned in a tubular furnace at 550 °C for 10 h. The as-obtained sodium oxide residue was dissolved in HCl for inductively coupled plasma (ICP) spectroscopic analysis (ICP) on a Thermo Fisher Scientific iCAP6300 spectrometer.

■ RESULTS AND DISCUSSION

PTCDI and its derivatives have been extensively investigated as n-channel semiconductor for organic optoelectronic applications because of their high electron affinity and large electron mobility in the solid state.[24] However, the electrochemical property of PTCDI as an organic Na-storage cathode remains unrevealed until now. To evaluate its cathodic performance, we ball-milled the PTCDI powders with conductive carbon under Ar protection so as to downsize the active particles and to establish well-connected electronic channels for electrochemical reactions.

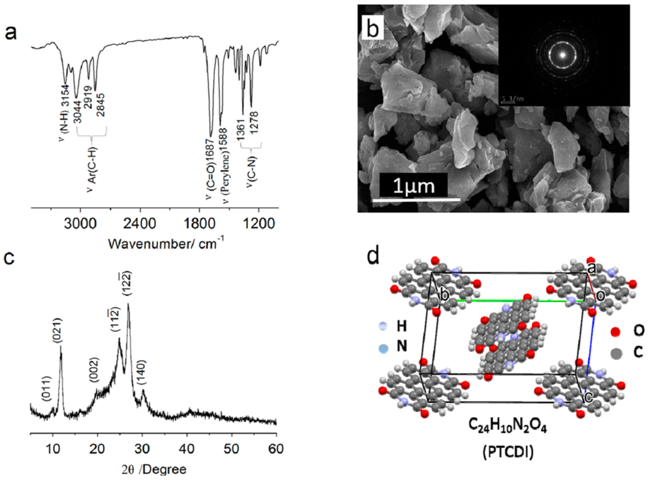

Figure 1. Structural characterizations of the PTCDI sample: (a) IR spectrum; (b) SEM image and SAED pattern (inset); (c) XRD pattern; and (d) schematic diagram of the molecular arrangement in PTCDI crystal.

The molecular structure of PTCDI was confirmed by FTIR spectrometry. As shown in Figure 1a, all the IR features can be assigned to the characteristic vibrations of perylene ring and imide groups of PTCDI structure. The absorption peaks at 3044, 2919, 2845, and 1588 cm^{-1} reflect the stretching vibrations of Ar(C−H) bonds and perylene ring, while the absorptions at 3154, 1687, 1361, and 1278 cm^{-1} correspond to the stretching vibrations of the N−H, C═O, and C−N bonds of imide groups, respectively. The IR pattern suggests that the PTCDI molecules kept their chemical structure untouched during ball-milling treatment. The particle morphology of the PTCDI sample was observed by scanning electron microscopy (SEM). As displayed in Figure 1b, the PTCDI sample appeared as irregularly shaped and unevenly sized powders with diameters ranging from 100 nm to 1 μm. The selected-area electron diffraction (SAED) in Figure 1b (inset) shows a ring-like pattern with many intense spots, revealing a polycrystalline structure of the PTCDI powders. The XRD pattern of PTCDI is given in Figure 1c. Compared with previous crystallographic analysis of PTCDI derivatives,[24−26] the XRD peaks in Figure 1c can be assigned to the (011), (021), (002), $(11\bar{2})$, $(12\bar{2})$, and (140) planes of PTCDI crystal (monoclinic P21/n space group), respectively. The molecular arrangement in this PTCDI crystal is schematically shown in Figure 1d. The PTCDAs are planar-stacked in a herringbone packing with the unite cell parameters of a = 4.865 Å, b = 14.66 Å, c = 10.84 Å, and β = 91.33°. The detailed crystal parameters of PTCDI are given in Supporting Information (Table S1).

Electrochemical performances of the PTCDI cathode were evaluated by cyclic voltammetry (CV) and galvanostatic discharge/charge measurements. Figure 2a shows the first two cycles of the CV curves of a PTCDI electrode in 1 mol L^{-1} $NaPF_6$ + EC/DEC/PC electrolyte. During the first cathodic scan, only one large reduction peak appears at a more negative potential of 1.6 V, suggesting a large polarization needed for initial electrochemical insertion of Na^+ ions into the uncoordinated PTCDI molecules. On the reversed anodic scan, two anodic peaks emerge at 2.30 and 2.80 V, respectively, corresponding to a two-stepped oxidation of $[C_{24}H_{10}N_2O_4]^{2-}$ → $[C_{24}H_{10}N_2O_4]^{-}$ → $[C_{24}H_{10}N_2O_4]$. Moreover, a small shoulder peak can also be observed at 2.62 V, probably due to a bond rearrangement of the PTCDI molecule at the positive potential. During subsequent cycles, these three pairs of redox

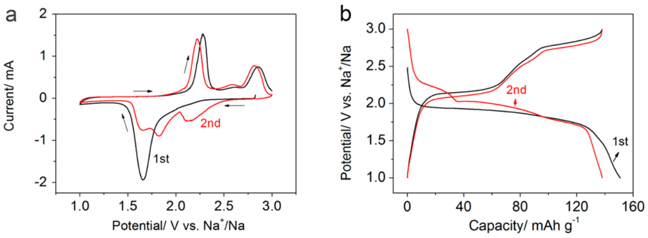

Figure 2. (a) CV curves of the PTCDI electrode measured at a scan rate of 1 mV s^{-1} and (b) charge/discharge profiles at a constant current of 10 mA g^{-1}.

peaks remained almost unchanged in their positions and intensities in the potential region of 3−1.5 V, implying a multiple electron transfer reaction and electrochemical reversibility of the cathodic reaction.

The charge/discharge profiles of the PTCDI electrode are in a close correspondence with its CV curves. As displayed in Figure 2b, there is only one voltage plateau at ∼1.7 V at first discharge of the PTCDI cathode, whereas there are three plateaus appearing at 2.0, 2.5, and 2.8 V during the first charge. Since the second cycle, the charge/discharge curves remained almost the same during successive cycles, confirming the electrochemical reversibility and cycling stability of the organic cathode. The first charge/discharge capacities of the PTCDI cathode are 150/140 mAh g^{-1}, corresponding to an initial Coulombic efficiency of 93.3%, which is even higher than those of inorganic Na^+-insertion cathodes. During subsequent cycles, the PTCDI cathode delivers stable charge/discharge capacities of 138.7/138.6 mAh g^{-1}, which correspond to a 2-electron redox capacity per PTCDI molecule (137 mAh g^{-1}). The slightly higher charge capacity (∼10 mAh g^{-1}) at the first cycle is most likely due to the formation of solid electrolyte interphase (SEI film) on the PTCDI cathode. According to previous investigations of the redox mechanism of aromatic imides in Li^+ electrolytes,[26−28] the charge/discharge reactions of imide compounds take place through an electrochemical enolization reaction of their carbonyl groups along with Li^+ ions associating with and disassociating from the oxygen atoms of the imide groups. In light of this redox mechanism, the redox reaction of the PTCDI cathode could be analogously assigned to a reversible enolization process, in which the carbonyl groups of the imide structure undergo electron transfer reaction accompanied by the insertion and extraction of Na^+ ions. In principle, each PTCDI molecule has four carbonyl groups, which should be able to transfer four electrons for reversible accommodation of 4 Na^+ ions. However, like the most of aromatic imides reported for Na^+ and Li^+ storage applications,[14,26−28] the PTCDI cathode can only realize a two-electron redox reaction at acceptably high potential of ≥1.5 V, possibly due to the electrostatic repulsion and steric hindrance in the PTCDI crystal. On the basis of the CV features and charge/discharge capacities, the redox mechanism of the PTCDI cathode could be described as a two-stepped enolization reaction with reversible insertion of 2 Na^+ ions, as shown in Scheme 1.

Scheme 1. Schematic Representation of the Proposed Redox Mechanism for Reversible Na Storage Reaction of PTCDI

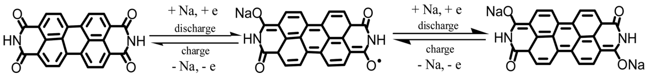

In addition to its 2 Na^+ storage capacity, the PTCDI cathode can also demonstrate a remarkable rate capability. Figure 3a shows the reversible capacities of the PTCDI electrode measured at various current rates from 20 mA g^{-1} (1/6 C) to 600 mA g^{-1} (5 C). As the current rate increased from 20 mA g^{-1} to 300 mA g^{-1} (2.5 C), the reversible capacity decreased slightly from 138 mAh g^{-1} to 118 mAh g^{-1}. Even at a very high rate of 600 mA g^{-1}, the PTCDI electrode can still deliver a quite high capacity of 103 mAh g^{-1}, which corresponds to a ∼75% capacity retention at such a high rate. When the current density was recovered to 200 mA g^{-1}, the reversible capacity returned to 116 mA h^{-1}, about 90% of its original value, demonstrating strong capacity retention of the PTCDI electrode. Such a high-rate performance is rarely seen for the most of organic electrode materials and is most likely due to the substantial electron mobility of the π-conjugated structure of PTCDI molecules and the large lamellar spacing of planar-stacked structure of PTCDI crystals, which facilitate electron transportation and Na^+ insertion into (or deinsertion from) the PTCDI lattice for charge/discharge reactions.

The long-term cycling performance of the PTCDI cathode was evaluated by galvanostatic cycling at a moderate current of 100 mA g^{-1}. As shown in Figure 3b, the reversible capacity of PTCDI electrode decreases very slightly from its initial value of 118.6 to 107 mAh g^{-1} after 300 cycles, corresponding to a capacity retention ratio of 90%. Usually, organic cathode materials are difficult to maintain a long cycle life due to their structural instability at high oxidation potentials and easy dissolution in organic electrolytes. In contrast, the long-term cycling stability of PTCDI is really very impressive, possibly due to the larger π-conjugated structure and strong intermolecular H-bonding of PTCDI molecules, which ensure the structural stability of PTCDI skeletons during repeated charge/discharge cycling.

To further confirm the Na^+-storage reaction mechanism, the changes in the bonding state, lattice structure and Na content of the PTCDI crystal cycled at different charge/discharge depths were characterized by FTIR, XRD and ICP analysis. Figure 4b shows the changes in the IR signals of the PTCDI electrode at different charge/discharge states. When first discharged to 2.0 V, the characteristic IR peak of the C═O stretching (1687 cm^{-1}) was widened and negatively shifted to 1623 cm^{-1}, suggesting that electrons were transferred into the C═O bonds, leading to a weakening of the C═O bonds. Meanwhile, the absorption peak at 1345 cm^{-1} from the C−N stretching vibration increased its intensity, possibly because the electron transfer into the C═O bond would result in an increase in the dipole moment of adjacent C−N bond. When further discharged to 1.75 V, all the IR absorptions of perylene ring and imide C−N bond kept almost unchanged, while the C═O bond stretching at 1623 cm^{-1} was further shifted to 1619 cm^{-1}, reflecting a continuous reduction of the C═O groups. As fully discharged to 1.0 V, the IR absorption of the C═O bond became much weaker but still detectable, which agrees well with expectation from the discharge mechanism, as displayed in Scheme 1, that half of the C═O bonds would be enolized to convert into Na^+ enolate. As a result, the reduction of the C═O bonds leads to a decreased π-conjugation in the PTCDI structure, as reflected by a large shift of the perylene ring stretching vibration from 1588 to 1540 cm^{-1}. On the reversed charge, all the IR bands of the C═O, C−N and perylene ring reversibly regain their original positions and

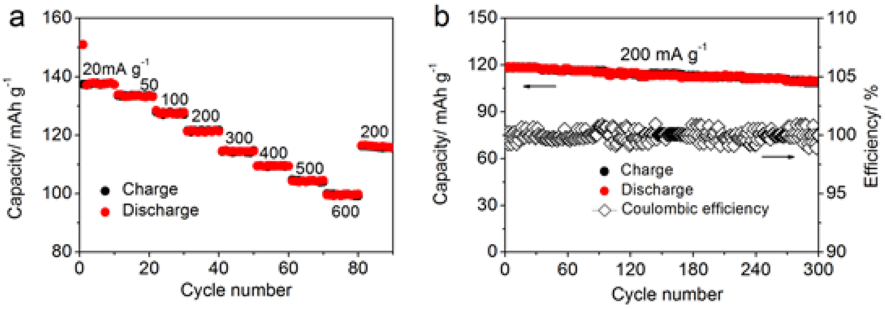

Figure 3. (a) Reversible capacities of PTCDI cycled at various rates as labeled and (b) long-term cycling stability at a constant current of 200 mA g^{-1}. The cells were cycled between the voltage interval of 3.0−1.0 V.

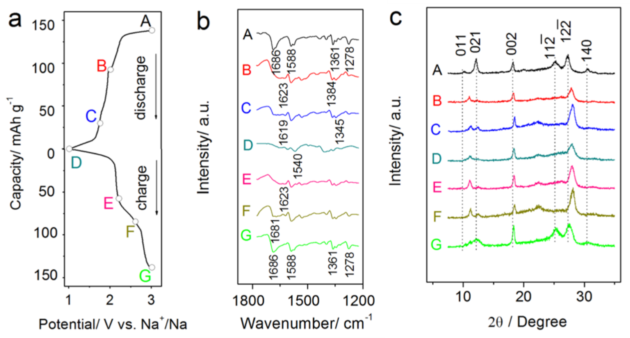

Figure 4. (a) A typical charge/discharge profile of the PTCDI cathode, where Arabic characters denote the sampling points. (b) IR spectra and (c) XRD patterns of the PTCDI electrode cycled at the selected potentials as indicated on each curve.

intensities, exhibiting a reversible change in the bonding states of PTCDI during charge and discharge.

In accord with the IR results, XRD analysis also reveals a reversible change of the PTCDI structure in the charge/discharge processes. As shown in Figure 4c, all the XRD peaks at 2θ = 10.15, 12.16, 25.08, 27.20, and 30.53° continuously decreased their intensities and finally disappeared with increasing depth of discharge, suggesting a structural breakdown of the PTCDI framework. Meanwhile, two new peaks at 2θ = 11.26 and 28.51° appeared and grew notably as the discharge proceeded. These phenomena suggest that the molecular arrangement pattern in the PTCDI crystal was changed when the Na^+ ions were inserted and associated with the carbonyl groups, which altered the original monoclinic symmetry of the PTCDI crystal. Nevertheless, all the XRD peaks can recover their original positions and intensities after charging, indicating a structural rearrangement from the Na^+-doped state to its pristine state. This reversible change of the XRD pattern further confirms the reversible phase transformation and structural stability of PTCDI in charge−discharge cycling.

ICP analysis of the Na^+ contents in the PTCDI cathode at different charge/discharge depths provides a direct evidence for the proposed Na insertion/extraction mechanism in Scheme 1. As given in Table S1 (Supporting Information), the Na^+ content in the PTCDI cathode increased from 0% at open circuit potential to 4.77 wt % at discharge potential of 2.0 V and finally to 10.48 wt % at discharge end potential of 1.0 V during discharge, which corresponds to the insertion of 1.98 Na^+ ions into each PTCDI molecule after a full discharge. On the reversed charging process, the Na content decreased from 10.48 wt % in the fully sodiated PTCDI to 0.07% in the fully charged state, demonstrating an almost complete removal of Na^+ ions from the discharged PTCDI cathode. This quantitative determination of Na^+ content in the cycled cathode not only confirms the 2Na-insertion mechanism but also explains the very high charge/discharge efficiency of PTCDI material. Such a high Coulombic efficiency plays a critical role for the PTCDI cathode to achieve a long-term cycling stability.

CONCLUSIONS

In summary, we selected a pristine perylene diimide, 3,4,9,10-perylene-bis(dicarboximide) (PTCDI), as a model compound to examine its Na-storage property. Benefiting from its high density of cathode-active and Na^+-associable carbonyl groups, the PTCDI molecule can undergo electrochemical enolization reaction with reversible insertion/extraction of 2 Na^+ ions per molecular unit, delivering a redox capacity of 140 mAh g^{-1} at 20 mA g^{-1} (1/6 C). In addition, this organic cathode also demonstrates a strong rate capability with a reversible capacity of 103 mAh g^{-1} at 600 mA g^{-1} (5 C) and a stable cyclability with 90% capacity retention over 300 cycles. Particularly, this PTCDI material is commercially available, low-cost, and nontoxic, and thus, it may serve as a new alternative cathode for Na-ion battery applications.

ASSOCIATED CONTENT

Supporting Information

The Supporting Information is available free of charge on the ACS Publications website at DOI: 10.1021/acsami.5b04325.

Crystal parameters of PTCDI and ICP analysis of the Na^+ content in the PTCDI electrodes at different depths of charge and discharge. (PDF)

AUTHOR INFORMATION

Corresponding Author

* E-mail: hxyang@whu.edu.cn. Tel: +86-27-68754526.

Author Contributions

The manuscript was written through contributions of all authors. All authors have given approval to the final version of the manuscript.

Notes

The authors declare no competing financial interest.

■ ACKNOWLEDGMENTS

This work is financially supported by the National Science Foundation of China (2133307) and the National 973 program of China (2015CB251100).

■ REFERENCES

(1) Slater, M. D.; Kim, D.; Lee, E.; Johnson, C. S. Sodium-Ion Batteries. *Adv. Funct. Mater.* **2013**, *23* (8), 947−958.

(2) Pan, H.; Hu, Y.-S.; Chen, L. Room-temperature Stationary Sodium-Ion Batteries for Large-scale Electric Energy Storage. *Energy Environ. Sci.* **2013**, *6* (8), 2338−2360.

(3) Palomares, V.; Serras, P.; Villaluenga, I.; Hueso, K. B.; Carretero-González, J.; Rojo, T. Na-ion batteries, Recent Advances and Present Challenges to become Low Cost Energy Storage Systems. *Energy Environ. Sci.* **2012**, *5* (3), 5884−5901.

(4) Kim, S. W.; Seo, D. H.; Ma, X.; Ceder, G.; Kang, K. Electrode Materials for Rechargeable Sodium-Ion Batteries: Potential Alternatives to Current Lithium-Ion Batteries. *Adv. Energy Mater.* **2012**, *2* (7), 710−721.

(5) Palomares, V.; Casas-Cabanas, M.; Castillo-Martínez, E.; Han, M. H.; Rojo, T. Update on Na-based Battery Materials. A Growing Research Path. *Energy Environ. Sci.* **2013**, *6* (8), 2312−2337.

(6) Song, Z.; Zhou, H. Towards Sustainable and Versatile Energy Storage Devices: an Overview of Organic Electrode Materials. *Energy Environ. Sci.* **2013**, *6* (8), 2280−2301.

(7) Zhao, R.; Zhu, L.; Cao, Y.; Ai, X.; Yang, H. X. An Aniline-NitroanilineCopolymer as a High Capacity Cathode for Na-ion Batteries. *Electrochem. Commun.* **2012**, *21*, 36−38.

(8) Zhou, M.; Xiong, Y.; Cao, Y.; Ai, X.; Yang, H. Electroactive Organic Anion-Doped Polypyrrole as a Low Cost and Renewable Cathode for Sodium-Ion Batteries. *J. Polym. Sci., Part B: Polym. Phys.* **2013**, *51* (2), 114−118.

(9) Zhou, M.; Zhu, L.; Cao, Y.; Zhao, R.; Qian, J.; Ai, X.; Yang, H. Fe $(CN)_6^{4-}$-Doped Polypyrrole: a High-Capacity and High-Rate Cathode Material for Sodium-Ion Batteries. *RSC Adv.* **2012**, *2* (13), 5495−5498.

(10) Han, S. C.; Bae, E. G.; Lim, H.; Pyo, M. Non-Crystalline Oligopyrene as a Cathode Material with a High-Voltage Plateau for Sodium Ion Batteries. *J. Power Sources* **2014**, *254*, 73−79.

(11) Deng, W.; Liang, X.; Wu, X.; Qian, J.; Cao, Y.; Ai, X.; Feng, J.; Yang, H. A Low Cost, All-Organic Na-ion Battery Based on Polymeric Cathode and Anode. *Sci. Rep.* **2013**, 3. DOI: 10.1038/srep02671

(12) Shen, Y.; Yuan, D.; Ai, X.; Yang, H.; Zhou, M. Poly (Diphenylaminesulfonic Acid Sodium) as a Cation-Exchanging Organic Cathode for Sodium Batteries. *Electrochem. Commun.* **2014**, *49*, 5−8.

(13) Zhu, L.; Shen, Y.; Sun, M.; Qian, J.; Cao, Y.; Ai, X.; Yang, H. Self-Doped Polypyrrole with Ionizable Sodium Sulfonate as a Renewable Cathode Material for Sodium Ion Batteries. *Chem. Commun.* **2013**, *49* (97), 11370−11372.

(14) Wang, H. g.; Yuan, S.; Ma, D. l.; Huang, X. l.; Meng, F. l.; Zhang, X. b., Tailored Aromatic Carbonyl Derivative Polyimides for High-Power and Long-Cycle Sodium-Organic Batteries. *Adv. Energy Mater.* **2014**, *4* (7). DOI: 10.1002/aenm.201301651

(15) Banda, H.; Damien, D.; Nagarajan, K.; Hariharan, M.; Shaijumon, M. M. A Polyimide based All-Organic Sodium Ion Battery. *J. Mater. Chem. A* **2015**, 3, 10453−10458.

(16) Liang, Y.; Zhang, P.; Chen, J. Function-Oriented Design of Conjugated Carbonyl Compound Electrodes for High Energy Lithium Batteries. *Chem. Sci.* **2013**, *4* (3), 1330−1337.

(17) Liang, Y.; Zhang, P.; Yang, S.; Tao, Z.; Chen, J. Fused Heteroaromatic Organic Compounds for High-Power Electrodes of Rechargeable Lithium Batteries. *Adv. Energy Mater.* **2013**, 3 (5), 600−605.

(18) Liang, Y.; Tao, Z.; Chen, J. Organic Electrode Materials for Rechargeable Lithium Batteries. *Adv. Energy Mater.* **2012**, 2 (7), 742−769.

(19) Kim, D. J.; Je, S. H.; Sampath, S.; Choi, J. W.; Coskun, A. Effect of N-substitution in Naphthalenediimides on the Electrochemical Performance of Organic Rechargeable Batteries. *RSC Adv.* **2012**, *2*, 7968−7970.

(20) Yao, M.; Kuratani, K.; Kojima, T.; Takeichi, N.; Senoh, H.; Kiyobayashi, T., Indigo Carmine: An Organic Crystal as a Positive-Electrode Material for Rechargeable Sodium Batteries. *Sci. Rep.* **2014**, *4*. DOI: 10.1038/srep03650

(21) Renault, S.; Mihali, V. A.; Edström, K.; Brandell, D. Stability of Organic Na-ion battery electrode materials: The Case of Disodium Pyromellitic Diimidate. *Electrochem. Commun.* **2014**, *45*, 52−55.

(22) Luo, W.; Allen, M.; Raju, V.; Ji, X., An Organic Pigment as a High-Performance Cathode for Sodium-Ion Batteries. *Adv. Energy Mater.* **2014**, *4* (15). DOI: 10.1002/aenm.201400554

(23) Macrae, C. F.; Bruno, I. J.; Chisholm, J. A.; Edgington, P. R.; McCabe, P.; Pidcock, E.; Rodriguez-Monge, L.; Taylor, R.; van de Streek, J.; Wood, P. A. Mercury CSD 2.0−New Features for the Visualization and Investigation of Crystal Structures. *J. Appl. Crystallogr.* **2008**, *41* (2), 466−470.

(24) Delgado, M. C. R.; Kim, E.-G.; Filho, D. t. A. d. S.; Bredas, J.-L. Tuning the Charge-Transport Parameters of Perylene Diimide Single Crystals via End and/or Core Functionalization: a Density Functional Theory Investigation. *J. Am. Chem. Soc.* **2010**, *132* (10), 3375−3387.

(25) Klebe, G.; Graser, F.; Hädicke, E.; Berndt, J. Crystallochromy as a Solid-State Effect: Correlation of Molecular Conformation, Crystal Packing and Colour in Perylene-3, 4:9, 10-Dis (Dicarboximide) Pigments. *Acta Crystallogr., Sect. B: Struct. Sci.* **1989**, *45* (1), 69−77.

(26) Han, X.; Chang, C.; Yuan, L.; Sun, T.; Sun, J. Aromatic Carbonyl Derivative Polymers as High-Performance Li-Ion Storage Materials. *Adv. Mater.* **2007**, *19* (12), 1616−1621.

(27) Wu, H.; Wang, K.; Meng, Y.; Lu, K.; Wei, Z. An Organic Cathode Material Based on a Polyimide/CNT Nanocomposite for Lithium Ion Batteries. *J. Mater. Chem. A* **2013**, *1* (21), 6366−6372.

(28) Song, Z.; Zhan, H.; Zhou, Y. Polyimides: Promising Energy-Storage Materials. *Angew. Chem.* **2010**, *122* (45), 8622−8626.